Predictions for the Dirac Phase in the Neutrino Mixing Matrix and Sum Rules

Journal of Physics: Conference Series **631** (2015) 012051 doi:10.1088/1742-6596/631/1/012051

Predictions for the Dirac Phase in the Neutrino Mixing Matrix and Sum Rules

I. Girardi[a)] [1], **S. T. Petcov**[a,b)] [2], **A. V. Titov**[a)]

[a] SISSA/INFN, Via Bonomea 265, 34136 Trieste, Italy

[b] Kavli IPMU (WPI), University of Tokyo, 5-1-5 Kashiwanoha, 277-8583 Kashiwa, Japan

Abstract. Using the fact that the neutrino mixing matrix $U = U_e^\dagger U_\nu$, where U_e and U_ν result from the diagonalisation of the charged lepton and neutrino mass matrices, we analyse the sum rules which the Dirac phase δ present in U satisfies when U_ν has a form dictated by, or associated with, discrete symmetries and U_e has a "minimal" form (in terms of angles and phases it contains) that can provide the requisite corrections to U_ν, so that reactor, atmospheric and solar neutrino mixing angles θ_{13}, θ_{23} and θ_{12} have values compatible with the current data. The following symmetry forms are considered: i) tri-bimaximal (TBM), ii) bimaximal (BM) (or corresponding to the conservation of the lepton charge $L' = L_e - L_\mu - L_\tau$ (LC)), iii) golden ratio type A (GRA), iv) golden ratio type B (GRB), and v) hexagonal (HG). We investigate the predictions for δ in the cases of TBM, BM (LC), GRA, GRB and HG forms using the exact and the leading order sum rules for $\cos\delta$ proposed in the literature, taking into account also the uncertainties in the measured values of $\sin^2\theta_{12}$, $\sin^2\theta_{23}$ and $\sin^2\theta_{13}$. This allows us, in particular, to assess the accuracy of the predictions for $\cos\delta$ based on the leading order sum rules and its dependence on the values of the indicated neutrino mixing parameters when the latter are varied in their respective 3σ experimentally allowed ranges.

1. Introduction

One of the major goals of the future experimental studies in neutrino physics is the searches for CP violation (CPV) effects in neutrino oscillations (see, e.g., [1, 2]). It is part of a more general and ambitious program of research aiming to determine the status of the CP symmetry in the lepton sector.

In the case of 3-neutrino mixing reference scheme and massive Majorana neutrinos we are going to consider, the CP symmetry can be violated in the lepton sector by the presence of one Dirac and two Majorana [3] CPV phases in the 3×3 unitary Pontecorvo, Maki, Nakagawa and Sakata (PMNS) neutrino mixing matrix. If the Dirac phase δ has a CP-non-conserving value, i.e., if $\delta \neq 0, \pi$, this will induce, as is well known, CPV effects in neutrino oscillations,

[1] Talk given by the author at DISCRETE 2014, 3 December 2014, London, England.

[2] Also at: Institute of Nuclear Research and Nuclear Energy, Bulgarian Academy of Sciences, 1784 Sofia, Bulgaria.

i.e., the CP-violating asymmetry $A_{\rm CP}^{l,l'} \equiv P(\nu_l \to \nu_{l'}) - P(\bar{\nu}_l \to \bar{\nu}_{l'})$, $l \neq l' = e, \mu, \tau$, for neutrino oscillations in vacuum, will be different from zero. Here $P(\nu_l \to \nu_{l'})$ and $P(\bar{\nu}_l \to \bar{\nu}_{l'})$, $l, l' = e, \mu, \tau$, are the flavour neutrino oscillation probabilities, which do not depend on the Majorana phases as was shown in [3, 4].

In the present study we will be concerned with predictions for the Dirac phase δ. More specifically, we will be interested in the predictions for the Dirac CPV phase δ which are based on the so-called "sum rules" for $\cos\delta$ [5–7] (see also, e.g., [8–10]). The sum rules of interest appear in an approach aiming at quantitative understanding of the pattern of neutrino mixing on the basis of symmetry considerations. In this approach one exploits the fact that, up to perturbative corrections, the PMNS matrix has an approximate form, U_ν, which can be dictated by symmetries. The matrix U_ν is assumed to originate from the diagonalisation of the neutrino Majorana mass term [3]. The angles in U_ν have specific symmetry values which differ, in general, from the experimentally determined values of the PMNS angles θ_{12}, θ_{13} and θ_{23}, and thus need to be corrected. The requisite perturbative corrections, which modify the values of the angles in U_ν to coincide with the measured values of θ_{12}, θ_{13} and θ_{23}, are provided by the matrix U_e arising from the diagonalisation of the charged lepton mass matrix, $U = U_e^\dagger\, U_\nu$. In the sum rules we will analyse in detail the Dirac phase δ, more precisely, $\cos\delta$, is expressed, in general, in terms of the mixing angles θ_{12}, θ_{13} and θ_{23} of the PMNS matrix U and the angles present in U_ν, whose values are fixed, being dictated by an underlying approximate discrete symmetry of the lepton sector (see, e.g., [9]).

A more detailed analysis can be found in ref. [11], on which this contribution is based.

2. The Sum Rules

In the framework of the reference 3 flavour neutrino mixing we will consider, the PMNS neutrino mixing matrix is always given by

$$U = U_e^\dagger U_\nu\,, \tag{1}$$

where U_e and U_ν are 3×3 unitary matrices originating from the diagonalisation of the charged lepton and the neutrino (Majorana) mass terms. As we have already indicated, we will suppose in what follows that U_ν has a form which is dictated by symmetries. More specifically, we will assume that

$$U_\nu = \Psi_1\, \tilde{U}_\nu\, Q_0 = \Psi_1\, R_{23}\,(\theta_{23}^\nu)\, R_{12}\,(\theta_{12}^\nu)\, Q_0\,, \tag{2}$$

where $R_{23}(\theta_{23}^\nu)$ and $R_{12}(\theta_{12}^\nu)$ are orthogonal matrices describing clockwise rotations in the 2-3 and 1-2 planes, respectively, and Ψ_1 and Q_0 are diagonal phase matrices each containing two phases. Obviously, the phases in the matrix Q_0 give contribution to the Majorana phases in the PMNS matrix. We will consider the following symmetry forms of the matrix $\tilde{U}_\nu$: i) tri-bimaximal (TBM) [12], ii) bimaximal (BM), or due to a symmetry corresponding to the conservation of the lepton charge $L' = L_e - L_\mu - L_\tau$ (LC) [13, 14], iii) golden ratio type A (GRA) form [15, 16], iv) golden ratio type B (GRB) form [17], and v) hexagonal (HG) form [18, 19]. The TBM, BM, GRA, GRB and HG forms can be obtained respectively from, e.g., T', A_4, A_5, D_{10} and D_{12} discrete (lepton) flavour symmetries (see, e.g., [9, 15–17, 19–21]).

[3] It is worth noticing that, since we are not interested in the predictions for the Majorana phases in this work, the results we are going to present will be valid also in the case of Dirac massive neutrinos.

In all these cases we have $\theta^{\nu}_{23} = -\pi/4$, and the matrix $\tilde{U}_{\nu}$ is given by

$$\tilde{U}_{\nu} = \begin{pmatrix} \cos\theta^{\nu}_{12} & \sin\theta^{\nu}_{12} & 0 \\ -\frac{\sin\theta^{\nu}_{12}}{\sqrt{2}} & \frac{\cos\theta^{\nu}_{12}}{\sqrt{2}} & -\frac{1}{\sqrt{2}} \\ -\frac{\sin\theta^{\nu}_{12}}{\sqrt{2}} & \frac{\cos\theta^{\nu}_{12}}{\sqrt{2}} & \frac{1}{\sqrt{2}} \end{pmatrix} . \tag{3}$$

The TBM, BM (LC), GRA, GRB and HG forms of $\tilde{U}_{\nu}$ correspond to different fixed values of θ^{ν}_{12} and thus of $\sin^2\theta^{\nu}_{12}$, namely, to i) $\sin^2\theta^{\nu}_{12} = 1/3$, ii) $\sin^2\theta^{\nu}_{12} = 1/2$, iii) $\sin^2\theta^{\nu}_{12} = (2+r)^{-1} \cong 0.276$, r being the golden ratio, $r = (1+\sqrt{5})/2$, iv) $\sin^2\theta^{\nu}_{12} = (3-r)/4 \cong 0.345$, and v) $\sin^2\theta^{\nu}_{12} = 1/4$. Thus, the matrix U_e in eq. (1) should provide corrections which not only generate non-zero value of θ_{13}, but also lead to reactor, atmospheric and solar neutrino mixing angles θ_{13}, θ_{23} and θ_{12} which have values compatible with the current data, including a possible sizeable deviation of θ_{23} from $\pi/4$. As was shown in [5], the "minimal" form of U_e, in terms of angles and phases it contains, that can provide the requisite corrections to U_{ν} includes a product of two orthogonal matrices describing clockwise rotations in the 2-3 and 1-2 planes, $R_{23}(\theta^{e}_{23})$ and $R_{12}(\theta^{e}_{12})$, θ^{e}_{23} and θ^{e}_{12} being two (real) angles [5]: $U_e = \Psi^{\dagger}_2 \tilde{U}_e = \Psi^{\dagger}_2 R^{-1}_{23}(\theta^{e}_{23}) R^{-1}_{12}(\theta^{e}_{12})$, where Ψ_2 is a diagonal phase matrix including two phases.

In the setting considered the PMNS matrix can be recast in the form [5]:

$$U = R_{12}(\theta^{e}_{12})\, \Phi(\phi)\, R_{23}(\hat{\theta}_{23})\, R_{12}(\theta^{\nu}_{12})\, \hat{Q}\,, \tag{4}$$

where $\phi = \arg(e^{-i\psi}\cos\theta^{e}_{23} + e^{-i\omega}\sin\theta^{e}_{23})$, $\sin^2\hat{\theta}_{23} = 1/2 - \sin\theta^{e}_{23}\cos\theta^{e}_{23}\cos(\omega-\psi)$, and $\hat{Q}$ is a diagonal phase matrix contributing to the Majorana phases.

From the comparison of the parametrisation of U, given in eq. (4), with the standard one [1], it follows that the four observables θ_{12}, θ_{23}, θ_{13} and δ are functions of three parameters θ^{e}_{12}, $\hat{\theta}_{23}$ and ϕ. As a consequence, the Dirac phase δ can be expressed as a function of the three PMNS angles θ_{12}, θ_{23} and θ_{13} [5], leading to a new "sum rule" relating δ and θ_{12}, θ_{23} and θ_{13}. For an arbitrary fixed value of the angle θ^{ν}_{12} the sum rules for $\cos\delta$ and $\cos\phi$ read [6]:

$$\sin^2\theta_{12} = \cos^2\theta^{\nu}_{12} + \frac{\sin 2\theta_{12}\sin\theta_{13}\cos\delta - \tan\theta_{23}\cos 2\theta^{\nu}_{12}}{\tan\theta_{23}(1 - \cot^2\theta_{23}\,\sin^2\theta_{13})}\,, \tag{5}$$

$$\sin^2\theta_{12} = \cos^2\theta^{\nu}_{12} + \frac{1}{2}\sin 2\theta_{23}\,\frac{\sin 2\theta^{\nu}_{12}\,\sin\theta_{13}\,\cos\phi - \tan\theta_{23}\cos 2\theta^{\nu}_{12}}{(1 - \cos^2\theta_{23}\,\cos^2\theta_{13})}\,. \tag{6}$$

Within the scheme considered the sum rules eqs. (5) – (6) are exact.

A parametrisation of the PMNS matrix, similar to that used by us, has been effectively employed in ref. [7]: the hierarchy of values of the angles in the matrices U_e and U_{ν} assumed in [7] leads the authors to consider the angles θ^{e}_{13} and θ^{ν}_{13} of the 1-3 rotations in U_e and U_{ν} as negligibly small. Treating $\sin\theta^{e}_{12}$ and $\sin\theta^{e}_{23}$ as small parameters, $|\sin\theta^{e}_{12}| \ll 1$, $|\sin\theta^{e}_{23}| \ll 1$, neglecting terms of order of, or smaller than, $O((\theta^{e}_{12})^2)$, $O((\theta^{e}_{23})^2)$ and $O(\theta^{e}_{12}\theta^{e}_{23})$, and taking into account that in this approximation we have $\sin\theta^{e}_{12} = \sqrt{2}\sin\theta_{13}$, the following "leading order" sum rule was obtained in [7]:

$$\theta_{12} \cong \theta^{\nu}_{12} + \theta_{13}\cos\delta\,. \tag{7}$$

This sum rule can be derived from the sum rule

$$\sin\theta_{12} \cong \sin\theta_{12}^{\nu} + \frac{\sin 2\theta_{12}^{\nu}}{2\sin\theta_{12}^{\nu}}\sin\theta_{13}\cos\delta\,, \tag{8}$$

by treating $\sin 2\theta_{12}^{\nu}\sin\theta_{13}\cos\delta \cong \sin 2\theta_{12}^{\nu}\theta_{13}\cos\delta$ as a small parameter and using the Taylor expansion $\sin^{-1}(a+b\,x) \cong \sin^{-1}(a) + b\,x/\sqrt{1-a^2}$, valid for $|bx| \ll 1$.

From eqs. (5) and (6), employing the approximations used in ref. [7], we get:

$$\sin^2\theta_{12} \cong \sin^2\theta_{12}^{\nu} + \sin 2\theta_{12}\sin\theta_{13}\cos\delta\,, \tag{9}$$

$$\sin^2\theta_{12} \cong \sin^2\theta_{12}^{\nu} + \sin 2\theta_{12}^{\nu}\,\sin\theta_{13}\,\cos\phi\,. \tag{10}$$

The first equation leads (in the leading order approximation used to derive it and using $\sin 2\theta_{12} \cong \sin 2\theta_{12}^{\nu}$) to eq. (7), while from the second equation we find

$$\sin\theta_{12} \cong \sin\theta_{12}^{\nu} + \frac{\sin 2\theta_{12}^{\nu}}{2\sin\theta_{12}^{\nu}}\sin\theta_{13}\cos\phi\,, \tag{11}$$

and correspondingly,

$$\theta_{12} \cong \theta_{12}^{\nu} + \theta_{13}\cos\phi\,. \tag{12}$$

This implies that in the leading order approximation adopted in ref. [7] we have [6] $\cos\delta \cong \cos\phi$. Note, however, that the sum rules for $\cos\delta$ and $\cos\phi$ given in eqs. (9) and (10), differ somewhat by the factors multiplying the terms $\sim \sin\theta_{13}$.

As was shown in [6], the leading order sum rule (7) leads in the cases of TBM, GRA, GRB and HG forms of $\tilde{U}_{\nu}$ to largely imprecise predictions for the value of $\cos\delta$: for the best fit values of $\sin^2\theta_{12} = 0.308$, $\sin^2\theta_{13} = 0.0234$ and $\sin^2\theta_{23} = 0.425$ used in [6], they differ approximately by factors (1.4 – 1.9) from the values found from the exact sum rule. The same result holds for $\cos\phi$. Moreover, the predicted values of $\cos\delta$ and $\cos\phi$ differ approximately by factors of (1.5 – 2.0), in contrast to the prediction $\cos\delta \cong \cos\phi$ following from the leading order sum rules. The large differences between the results for $\cos\delta$ and $\cos\phi$, obtained using the leading order and the exact sum rules, are a consequence [6] of the quantitative importance of the next-to-leading order terms which are neglected in the leading order sum rules (7) – (12). The next-to-leading order terms are significant for the TBM, GRA, GRB and HG forms of $\tilde{U}_{\nu}$ because in all these cases the "dominant" terms $|\theta_{12} - \theta_{12}^{\nu}| \sim \sin^2\theta_{13}$, or equivalently [4] $|\sin^2\theta_{12} - \sin^2\theta_{12}^{\nu}| \sim \sin^2\theta_{13}$. It was shown also in [6] that in the case of the BM (LC) form of $\tilde{U}_{\nu}$ we have $|\theta_{12} - \theta_{12}^{\nu}| \sim \sin\theta_{13}$ and the leading order sum rules provide rather precise predictions for $\cos\delta$ and $\cos\phi$.

A non-zero value of θ_{23}^{e} allows for a significant deviation of θ_{23} from $\pi/4$. Such deviation is not excluded by the current data on $\sin^2\theta_{23}$: at 3σ values of $\sin^2\theta_{23}$ in the interval (0.37 – 0.64) are allowed, the best fit value being $\sin^2\theta_{23} = 0.437$ (0.455) [22]. The exact sum rules for $\cos\delta$ and $\cos\phi$, eqs. (5) and (6), depend on θ_{23}, while the leading order sum rules, eqs. (7) and (12), are independent of θ_{23}. We are going to investigate how the dependence on θ_{23} affects the predictions for $\cos\delta$ and $\cos\phi$, based on the exact sum rules.

[4] Note that [6] since $\cos\delta$ and $\cos\phi$ in eqs. (7) – (12) are multiplied by $\sin\theta_{13}$, the "dominant" terms $|\theta_{12} - \theta_{12}^{\nu}|$ and the next-to-leading order terms $\sim \sin^2\theta_{13}$ give contributions to $\cos\delta$ and $\cos\phi$, which are both of the same order and are $\sim \sin\theta_{13}$.

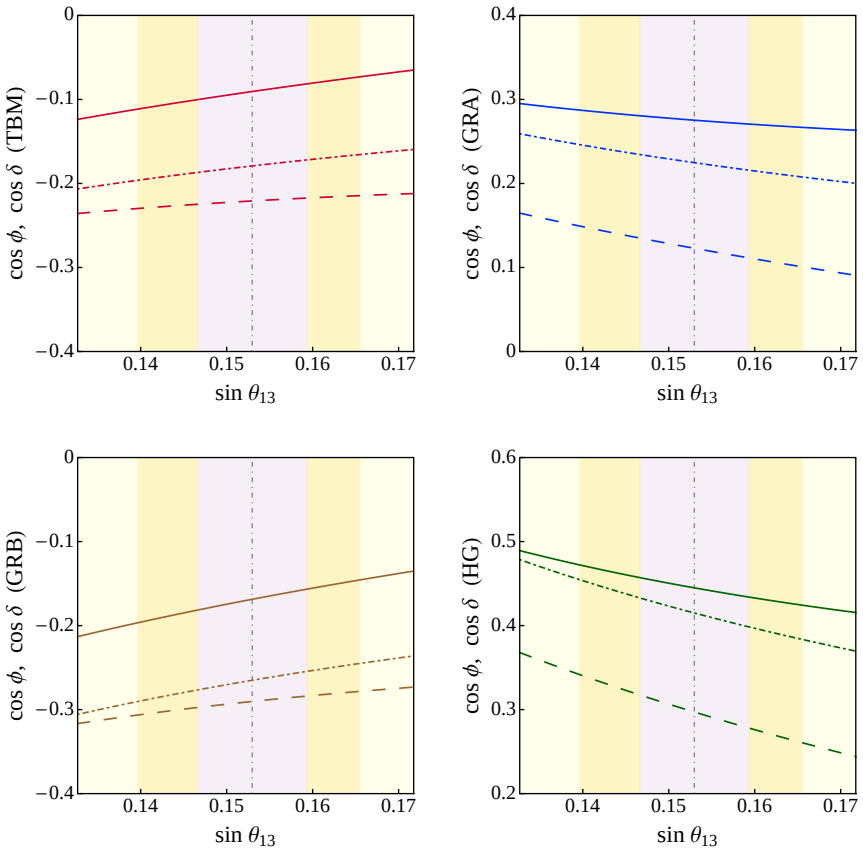

Figure 1: Predictions for $\cos\delta$ and $\cos\phi$ in the cases of the TBM (upper left panel), GRA (upper right panel), GRB (lower left panel) and HG (lower right panel) forms of the matrix $\tilde{U}_\nu$, as functions of $\sin\theta_{13}$ and for the best fit values of $\sin^2\theta_{12} = 0.308$ and $\sin^2\theta_{23} = 0.437$ [22]. The solid lines (dashed lines) correspond to $\cos\delta$ ($\cos\phi$) determined from the exact sum rule given in eq. (5) (eq. (6)). The dash-dotted line in each of the 4 panels represents $(\cos\delta)_{\rm LO} = (\cos\phi)_{\rm LO}$ obtained from the leading order sum rule in eq. (8) (eq. (11)). The vertical dash-dotted line corresponds to the best fit value of $\sin^2\theta_{13} = 0.0234$ [22]; the three coloured vertical bands indicate the 1σ, 2σ and 3σ experimentally allowed ranges of $\sin\theta_{13}$ (see text for further details).

We note first that from the exact sum rules in eqs. (5) and (6) we get to leading order in $\sin\theta_{13}$:

$$\sin^2\theta_{12} = \sin^2\theta^\nu_{12} + \frac{\sin 2\theta_{12}}{\tan\theta_{23}}\sin\theta_{13}\cos\delta + O(\sin^2\theta_{13})\,, \tag{13}$$

$$\sin^2\theta_{12} = \sin^2\theta^\nu_{12} + \frac{\sin 2\theta^\nu_{12}}{\tan\theta_{23}}\sin\theta_{13}\cos\phi + O(\sin^2\theta_{13})\,. \tag{14}$$

It follows that in the case of $|\sin\theta^e_{23}| \ll 1$ considered in ref. [7], we have [6] $\tan^{-1}\theta_{23} \cong 2\cos^2\theta_{23} = 1 + O(\sin\theta^e_{23})$. Applying the approximation employed in ref. [7], in which terms of the order of, or smaller than, $\sin^2\theta_{13}$, $\sin^2\theta^e_{23}$ and $\sin\theta_{13}\sin\theta^e_{23}$, in the sum rules of interest

$(\sin^2\theta_{12}, \sin^2\theta_{23}) = (0.308, 0.437)$	TBM	GRA	GRB	HG
$(\cos\delta)_{\rm E}$	-0.0906	0.275	-0.169	0.445
$(\cos\delta)_{\rm LO}$	-0.179	0.225	-0.265	0.415
$(\cos\delta)_{\rm E}/(\cos\delta)_{\rm LO}$	0.506	1.22	0.636	1.07
$(\cos\phi)_{\rm E}$	-0.221	0.123	-0.290	0.297
$(\cos\delta)_{\rm E}/(\cos\phi)_{\rm E}$	0.41	2.24	0.581	1.50
$(\cos\phi)_{\rm E}/(\cos\phi)_{\rm LO}$	1.23	0.547	1.10	0.716

Table 1: The predicted values of $\cos\delta$ and $\cos\phi$, obtained from the exact sum rules in eqs. (5) and (6), $(\cos\delta)_{\rm E}$ and $(\cos\phi)_{\rm E}$, and from the leading order sum rule in eq. (8) (eq. (11)), $(\cos\delta)_{\rm LO} = (\cos\phi)_{\rm LO}$, using the best fit values of $\sin^2\theta_{13} = 0.0234$, $\sin^2\theta_{12} = 0.308$ and $\sin^2\theta_{23} = 0.437$ [22], for the TBM, GRA, GRB and HG forms of the matrix $\tilde{U}_\nu$. The values of the ratios $(\cos\delta)_{\rm E}/(\cos\delta)_{\rm LO}$, $(\cos\delta)_{\rm E}/(\cos\phi)_{\rm E}$ and $(\cos\phi)_{\rm E}/(\cos\phi)_{\rm LO}$ are also shown.

are neglected, we have to set $\tan^{-1}\theta_{23} = 1$ in eqs. (13) and (14). This leads to eqs. (9) and (10) and, correspondingly, to eqs. (7) and (12).

In Fig. 1 we show the predictions for $\cos\delta$ and $\cos\phi$ in the cases of the TBM, GRA, GRB and HG forms of the matrix $\tilde{U}_\nu$, derived from the exact sum rules in eqs. (5) and (6), $(\cos\delta)_{\rm E}$ (solid line) and $(\cos\phi)_{\rm E}$ (dashed line), and from the leading order sum rule in eq. (8) (eq. (11)), $(\cos\delta)_{\rm LO} = (\cos\phi)_{\rm LO}$ (dash-dotted line). The results presented in Fig. 1 are obtained for the best fit values of $\sin^2\theta_{12} = 0.308$ and $\sin^2\theta_{23} = 0.437$ taken from [22]. The parameter $\sin^2\theta_{13}$ is varied in its 3σ allowed range. In Table 1 we give the values of $(\cos\delta)_{\rm E}$, $(\cos\delta)_{\rm LO}$, $(\cos\phi)_{\rm E}$ and of their ratios, corresponding to the best fit values of $\sin^2\theta_{12}$, $\sin^2\theta_{23}$ and $\sin^2\theta_{13}$. We see from Table 1 that for the TBM, GRA, GRB and HG forms of $\tilde{U}_\nu$, $\cos\delta$ determined from the exact sum rule takes respectively the values (-0.091), 0.275, (-0.169) and 0.445. The values of $\cos\delta$, found using the exact sum rule, eq. (5), differ in the TBM, GRA, GRB and HG cases from those calculated using the leading order sum rule, eq. (8), by the factors 0.506, 1.22, 0.636 and 1.07, respectively. Thus, the largest difference between the predictions of the exact and the leading order sum rules occurs for the TBM form of $\tilde{U}_\nu$.

Since the predictions of the sum rules depend on the value of θ_{12}, we show in Fig. 2 also results for the values of $\sin^2\theta_{12}$, corresponding to the lower bound of the 3σ allowed range of $\sin^2\theta_{12}$, $\sin^2\theta_{12} = 0.259$, keeping $\sin^2\theta_{23}$ fixed to its best fit value. The predictions for $(\cos\delta)_{\rm E}$, $(\cos\phi)_{\rm E}$, $(\cos\delta)_{\rm LO} = (\cos\phi)_{\rm LO}$ and their ratios, obtained for the best fit values of $\sin^2\theta_{13} = 0.0234$ and $\sin^2\theta_{23} = 0.437$, and for $\sin^2\theta_{12} = 0.259$ are given in Table 2. In this case the exact sum rule predictions of $\cos\delta$ for the TBM, GRA, GRB and HG forms of $\tilde{U}_\nu$ read (see Table 2): $(\cos\delta)_{\rm E} = (-0.408)$, (-0.022), (-0.490) and 0.156. The dependence of $(\cos\delta)_{\rm E}$, $(\cos\delta)_{\rm LO}$ and $(\cos\phi)_{\rm E}$ on $\sin^2\theta_{12}$ is shown graphically in Fig. 3.

Further, for $\sin^2\theta_{12} = 0.259$, the ratio $(\cos\delta)_{\rm E}/(\cos\delta)_{\rm LO}$ in the TBM, GRA, GRB and HG cases reads, respectively, 0.744, 0.172, 0.769 and 2.32 (see Table 2). Thus, the predictions for $\cos\delta$ of the exact and the leading order sum rules differ by the factors of 5.8 and 2.3 in the GRA and HG cases.

In what concerns the difference between the exact and leading order sum rules predictions for $\cos\delta$, for the best fit values of $\sin^2\theta_{13}$ and $\sin^2\theta_{12}$, and for $\sin^2\theta_{23} = 0.374$, the ratio $(\cos\delta)_{\rm E}/(\cos\delta)_{\rm LO} = 0.345$, 1.17, 0.494 and 0.993 for TBM, GRA, GRB and HG forms of $\tilde{U}_\nu$. For $\sin^2\theta_{23} = 0.626$, we have for the same ratio $(\cos\delta)_{\rm E}/(\cos\delta)_{\rm LO} = 1.04$, 1.52, 1.13 and 1.42.

Thus, for $\sin^2\theta_{23} = 0.374$ (0.626), the leading order sum rule prediction for $\cos\delta$ is rather precise in the HG (TBM) case. For the other symmetry forms of $\tilde{U}_\nu$ the leading order sum rule prediction for $\cos\delta$ is largely incorrect.

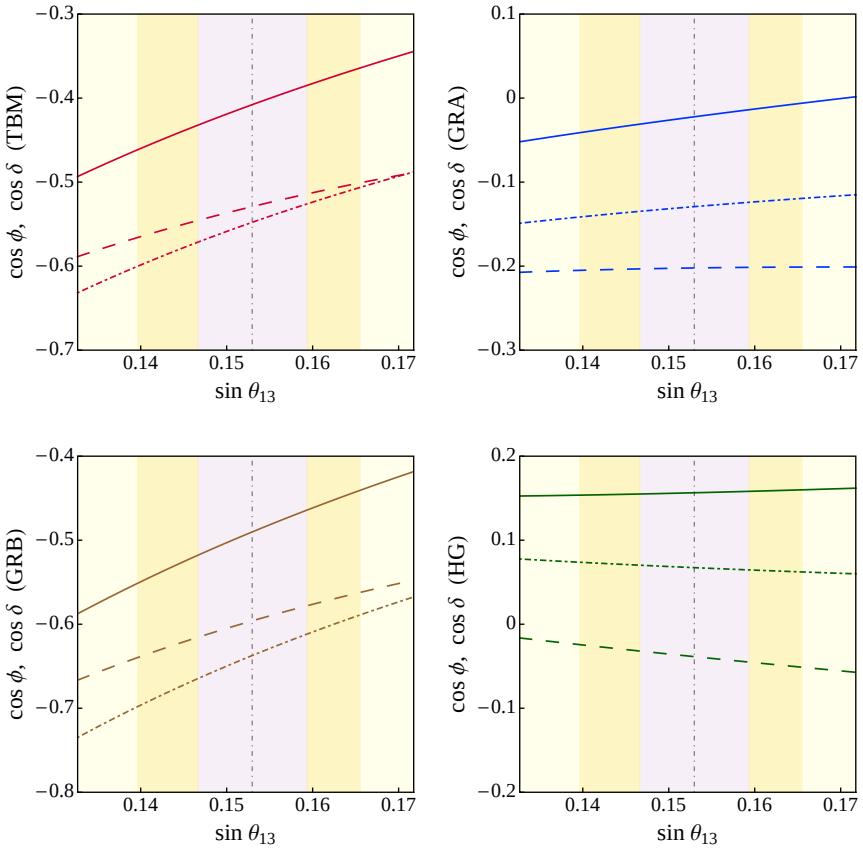

Figure 2: The same as in Fig. 1, but for $\sin^2\theta_{12} = 0.259$ (lower bound of the 3σ interval) and $\sin^2\theta_{23} = 0.437$ (best fit value) [22].

$(\sin^2\theta_{12}, \sin^2\theta_{23}) = (0.259, 0.437)$	TBM	GRA	GRB	HG
$(\cos\delta)_{\rm E}$	-0.408	-0.0223	-0.490	0.156
$(\cos\delta)_{\rm LO}$	-0.548	-0.129	-0.637	0.0673
$(\cos\delta)_{\rm E}/(\cos\delta)_{\rm LO}$	0.744	0.172	0.769	2.32
$(\cos\phi)_{\rm E}$	-0.529	-0.202	-0.596	-0.0386
$(\cos\delta)_{\rm E}/(\cos\phi)_{\rm E}$	0.771	0.110	0.822	-4.05
$(\cos\phi)_{\rm E}/(\cos\phi)_{\rm LO}$	0.966	1.57	0.935	-0.573

Table 2: The same as in Table 1, but for $\sin^2\theta_{13} = 0.0234$ (best fit value), $\sin^2\theta_{12} = 0.259$ (lower bound of the 3σ range) and $\sin^2\theta_{23} = 0.437$ (best fit value) [22].

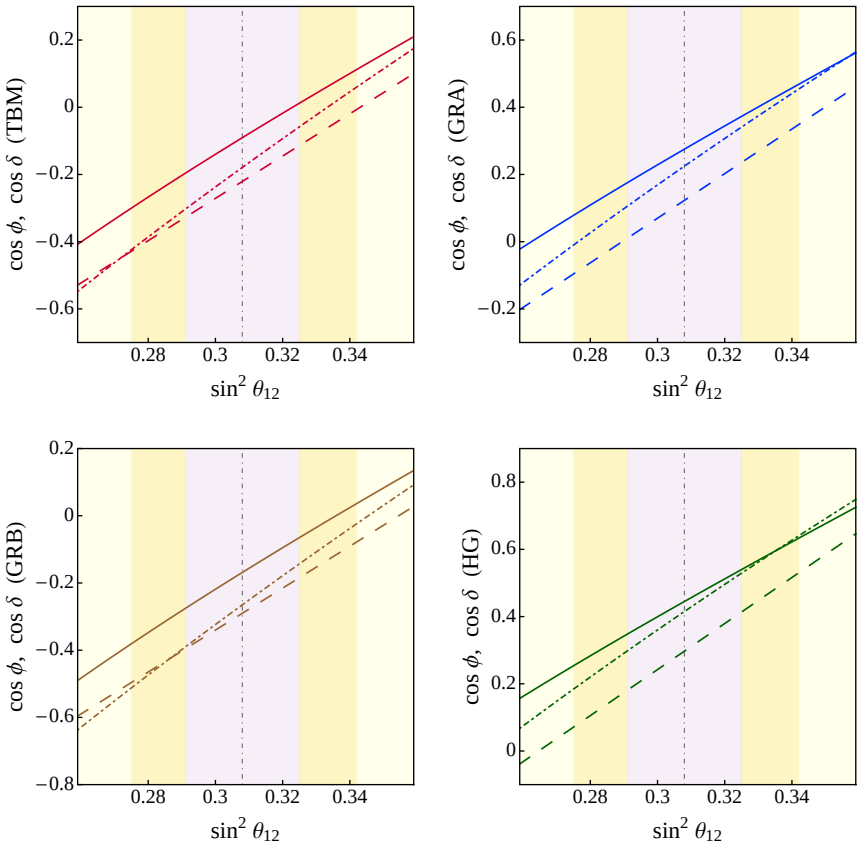

Figure 3: The same as in Fig. 1, but for $\sin^2\theta_{13} = 0.0234$, $\sin^2\theta_{23} = 0.437$ (best fit values) and varying $\sin^2\theta_{12}$ in the 3σ range. The vertical dash-dotted line corresponds to the best fit value of $\sin^2\theta_{12} = 0.308$ [22].

3. Statistical Analysis

We perform a statistical analysis of the predictions for δ, $\cos\delta$ and the rephasing invariant $J_{\rm CP}$ which controls the magnitude of CPV effects in neutrino oscillations [23], in the cases of the TBM, BM (LC), GRA, GRB and HG symmetry forms of the matrix $\tilde{U}_\nu$ (see eq. (3)). In this analysis we use as input the latest results on $\sin^2\theta_{12}$, $\sin^2\theta_{13}$, $\sin^2\theta_{23}$ and δ, obtained in the global analysis of the neutrino oscillation data performed in [22]. Our goal is to derive the allowed ranges for δ, $\cos\delta$ and $J_{\rm CP}$, predicted on the basis of the current data on the neutrino mixing parameters for each of the symmetry forms of $\tilde{U}_\nu$ considered. We recall that in the standard parametrisation of the PMNS matrix, the $J_{\rm CP}$ factor reads (see, e.g., [1]):

$$J_{\rm CP} = {\rm Im}\left\{U^*_{e1}U^*_{\mu 3}U_{e3}U_{\mu 1}\right\} = \frac{1}{8}\sin\delta\sin 2\theta_{13}\sin 2\theta_{23}\sin 2\theta_{12}\cos\theta_{13}\,. \qquad (15)$$

We construct χ^2 for the schemes considered — TBM, BM (LC), GRA, GRB and HG — as follows:

$$\chi^2(\sin^2\theta_{12},\sin^2\theta_{13},\sin^2\theta_{23},\delta) = \chi^2_1(\sin^2\theta_{12}) + \chi^2_2(\sin^2\theta_{13}) + \chi^2_3(\sin^2\theta_{23}) + \chi^2_4(\delta)\,, \qquad (16)$$

in which we have neglected the correlations among the oscillation parameters, since the functions χ^2_i have been extracted from the 1-dimensional projections in [22]. In order to quantify the accuracy of our approximation we show in Fig. 4 the confidence regions at 1σ, 2σ and 3σ for 1 degree of freedom in the planes $(\sin^2\theta_{23}, \delta)$, $(\sin^2\theta_{13}, \delta)$ and $(\sin^2\theta_{23}, \sin^2\theta_{13})$ in blue (dashed lines), purple (solid lines) and light-purple (dash-dotted lines) for NO (IO) neutrino mass spectrum, respectively, obtained using eq. (16). The parameters not shown in the plot have been marginalised. It should be noted that what is also used in the literature is

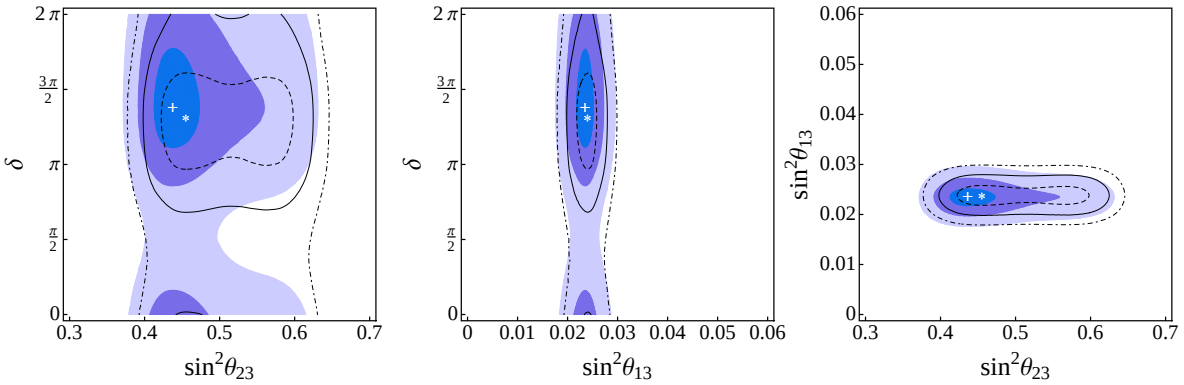

Figure 4: Confidence regions at 1σ, 2σ and 3σ for 1 degree of freedom in the planes $(\sin^2\theta_{23}, \delta)$, $(\sin^2\theta_{13}, \delta)$ and $(\sin^2\theta_{23}, \sin^2\theta_{13})$ in the blue (dashed lines), purple (solid lines) and light-purple (dash-dotted lines) for NO (IO) neutrino mass spectrum, respectively, obtained using eq. (16). The best fit points are indicated with a cross (NO) and an asterisk (IO).

the Gaussian approximation, in which χ^2 can be simplified using the best fit values and the 1σ uncertainties as follows:

$$\chi^2_{\rm G} = \sum_i \frac{(x_i - \overline{x}_i)^2}{\sigma^2_{x_i}} \,. \tag{17}$$

Here $x_i = \{\sin^2\theta_{12}, \sin^2\theta_{13}, \sin^2\theta_{23}, \delta\}$, $\overline{x}_i$ and σ_{x_i} being the best fit values and the 1σ uncertainties [5] taken from [22]. We present in Fig. 5 the results of a similar two-dimensional analysis for the confidence level regions in the planes shown in Fig. 4, but using the approximation for χ^2 given in eq. (17). It follows from these figures that the Gaussian approximation does not allow to reproduce the confidence regions of [22] with sufficiently good accuracy. For this reason in our analysis we use the more accurate procedure defined through eq. (16). In both the figures the best fit points are indicated with a cross and an asterisk for NO and IO spectra, respectively. Each symmetry scheme considered in our analysis, which we label with an index m, depends on a set of parameters y^m_j, which are related to the standard oscillation parameters x_i through expressions of the form $x_i = x^m_i(y^m_j)$. In order to produce the 1-dimensional figures we minimise χ^2 for a fixed value of the corresponding observable α, i.e., $\chi^2(\alpha) = \min[\chi^2(x^m_i(y^m_j))_{\alpha=\rm const}]$, with $\alpha = \{\delta, J_{\rm CP}\}$.

In the five panels in Fig. 6 we show $N_\sigma \equiv \sqrt{\chi^2}$ as a function of δ for the five symmetry forms of $\tilde{U}_\nu$ we have studied. The dashed lines correspond to the results of the global fit [22].

[5] In the case of asymmetric errors we take the mean value of the two errors.

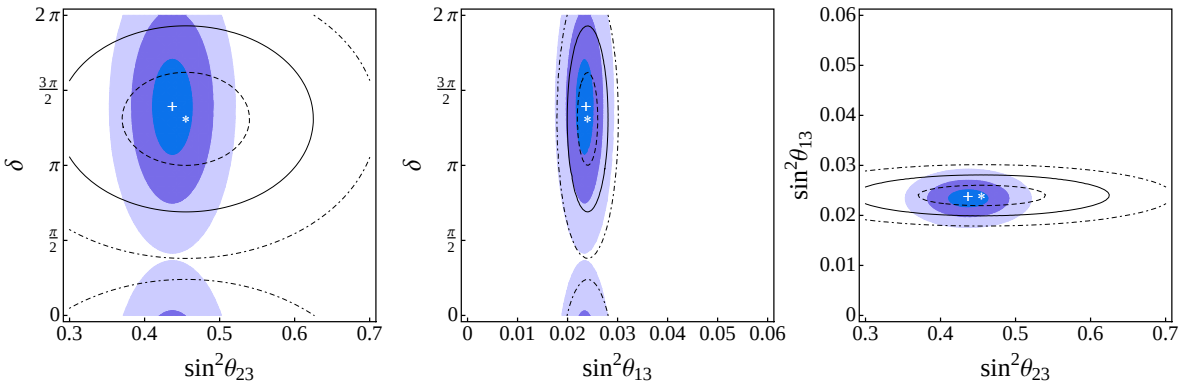

Figure 5: The same as in Fig. 4, but using eq. (17).

The solid lines represent the results we obtain by minimising the value of χ^2 in $\sin^2\theta_{13}$ and $\sin^2\theta_{23}$ (or, equivalently, in $\sin^2\theta^e_{12}$ and $\sin^2\hat{\theta}_{23}$) for a fixed value of δ [6]. The blue (red) lines correspond to NO (IO) neutrino mass spectrum. The value of χ^2 at the minimum, $\chi^2_{\rm min}$, which determines the best fit value of δ predicted for each symmetry form of $\tilde{U}_\nu$, allows us to make conclusions about the compatibility of a given symmetry form of $\tilde{U}_\nu$ with the current global neutrino oscillation data.

It follows from the results shown in Fig. 6 that the BM (LC) symmetry form is disfavoured by the data at approximately 1.8σ, all the other symmetry forms considered being compatible with the data. We note that for the TBM, GRA, GRB and HG symmetry forms, a value of δ in the vicinity of $3\pi/2$ is preferred statistically, in contrast, in the case of the BM (LC) form the best fit value is very close to π [5, 6, 11]. The somewhat larger value of χ^2 at the second local minimum in the vicinity of $\pi/2$ in the TBM, GRA, GRB and HG cases, is a consequence of the fact that the best fit value of δ obtained in the global analysis of the current neutrino oscillation data is close to $3\pi/2$ and that the value of $\delta = \pi/2$ is statistically disfavoured (approximately at 2.5σ). In the absence of any information on δ, the two minima would have exactly the same value of χ^2, because they correspond to the same value of $\cos\delta$. In the schemes considered, as we have discussed, $\cos\delta$ is determined by the values of θ_{12}, θ_{13} and θ_{23}. The degeneracy in the sign of $\sin\delta$ can only be solved by an experimental input on δ.

We have performed also a statistical analysis in order to derive predictions for $J_{\rm CP}$. In Fig. 7 we present $N_\sigma \equiv \sqrt{\chi^2}$ as a function of $J_{\rm CP}$ for NO and IO neutrino mass spectra. Similarly to the case of δ, we minimise the value of χ^2 for a fixed value of $J_{\rm CP}$ by varying $\sin^2\theta_{13}$ and $\sin^2\theta_{23}$ (or, equivalently, $\sin^2\theta^e_{12}$ and $\sin^2\hat{\theta}_{23}$). As Fig. 7 shows, the CP-conserving value of $J_{\rm CP} = 0$ is excluded in the cases of the TBM, GRA, GRB and HG neutrino mixing symmetry forms, respectively, at approximately 5σ, 4σ, 4σ and 3σ confidence levels with respect to the confidence level of the corresponding best fit values [7]. These results correspond to those we have obtained for δ, more specifically to the confidence levels at which the CP-conserving

[6] We note that in the scheme considered by us, fixing the value of δ implies that one of the three neutrino mixing angles is expressed in terms of the other two. We choose for convenience this angle to be θ_{12}.

[7] The confidence levels under discussion differ in the cases of NO and IO neutrino mass spectra, but as Fig. 7 indicates, in the cases considered these differences are rather small and we have not given them.

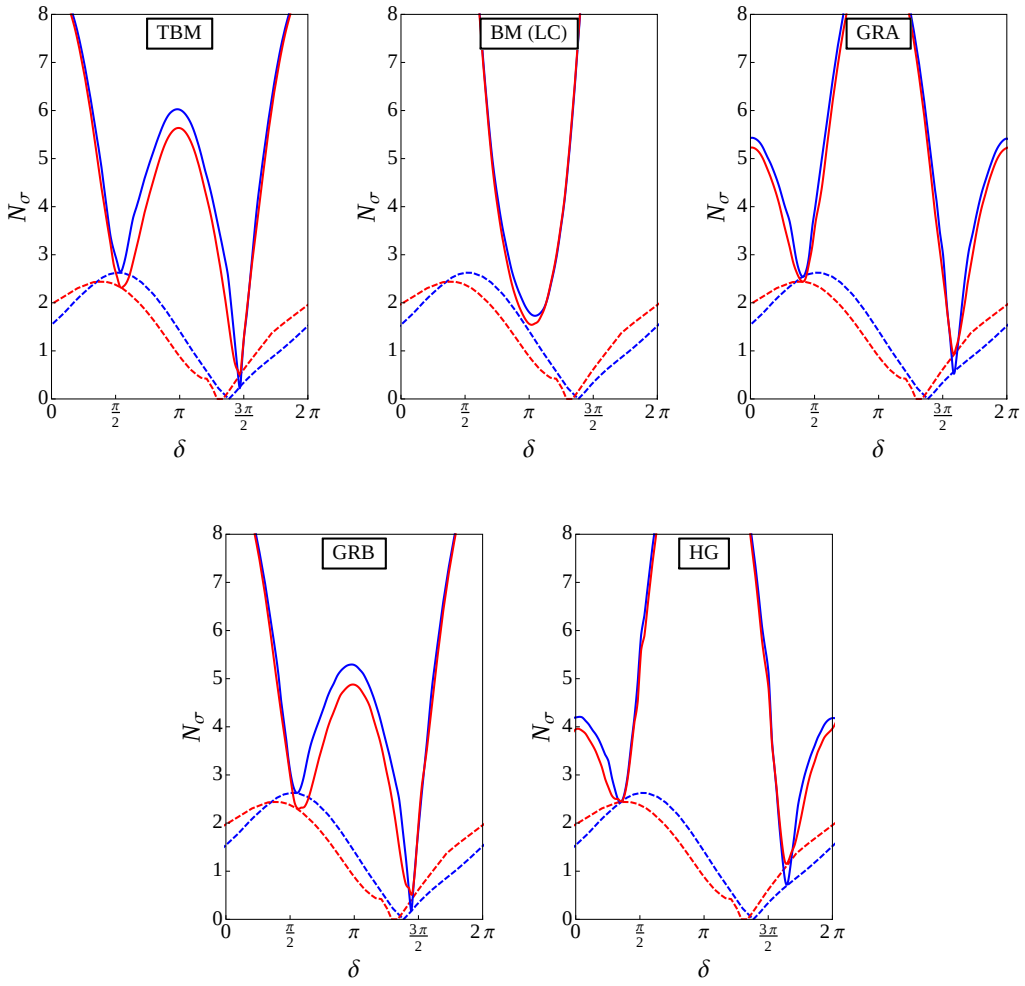

Figure 6: $N_\sigma \equiv \sqrt{\chi^2}$ as a function of δ. The dashed lines represent the results of the global fit [22], while the solid lines represent the results we obtain for the TBM, BM (LC), GRA (upper left, central, right panels), GRB and HG (lower left and right panels) symmetry forms of $\tilde{U}_\nu$. The blue (red) lines are for NO (IO) neutrino mass spectrum (see text for further details).

values of $\delta = 0$, π, 2π, are excluded (see Fig. 6).

In contrast, for the BM (LC) symmetry form, the CP-conserving value of δ, namely, $\delta \cong \pi$, is preferred and therefore the CPV effects in neutrino oscillations are predicted to be suppressed. At the best fit point we obtain a value of $J_{\rm CP} = -0.005$ (-0.002) for NO (IO) neutrino mass spectrum, which corresponds to the best fit value of $\delta/\pi = 1.04$ (1.02). The allowed range of the $J_{\rm CP}$ factor in the BM (LC) includes the CP-conserving value $J_{\rm CP} = 0$ at practically any confidence level. The tables which summarise the best fit values and the corresponding 3σ ranges for δ, $\cos\delta$, $J_{\rm CP}$ and $\sin^2\theta_{23}$ can be found in [11].

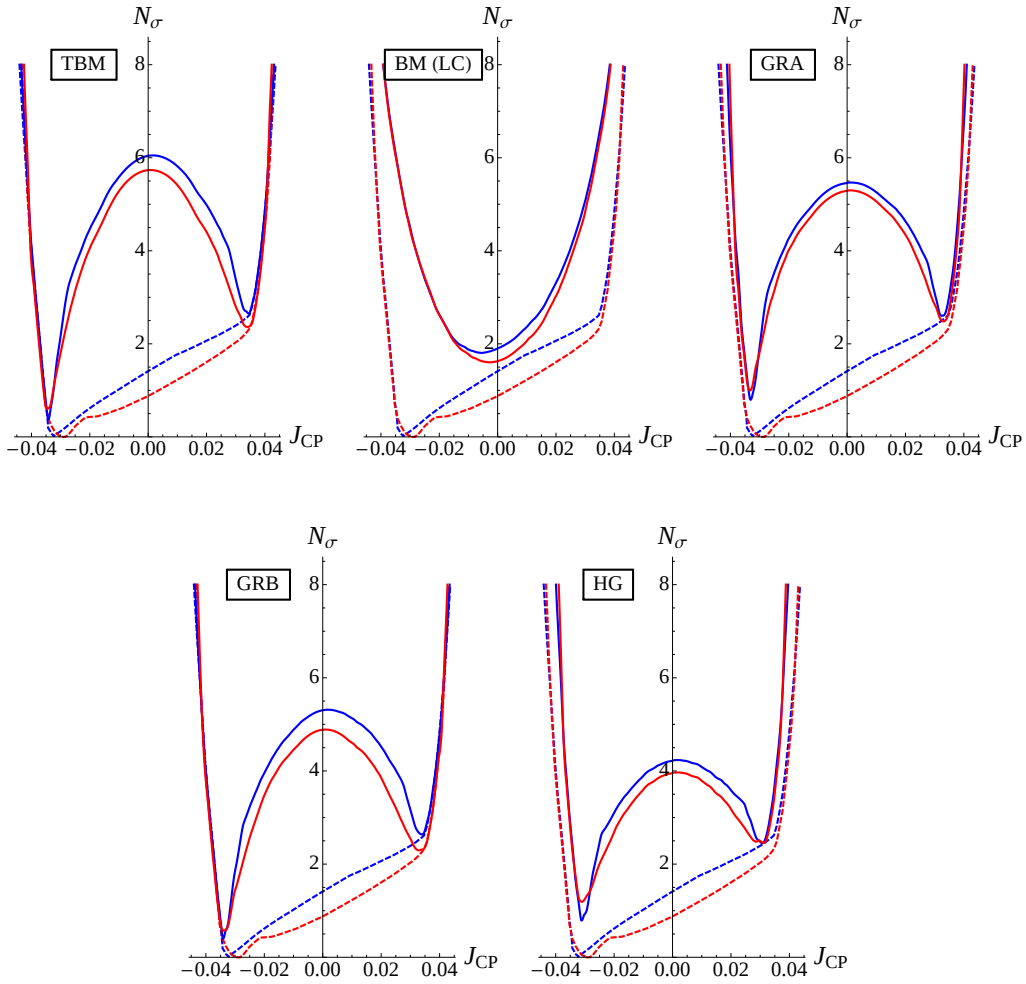

Figure 7: $N_\sigma \equiv \sqrt{\chi^2}$ as a function of $J_{\rm CP}$. The dashed lines represent the results of the global fit [22], while the solid lines represent the results we obtain for the TBM, BM (LC), GRA (upper left, central, right panels), GRB and HG (lower left and right panels) neutrino mixing symmetry forms. The blue (red) lines are for NO (IO) neutrino mass spectrum (see text for further details).

Summary and Conclusions

Using the fact that the neutrino mixing matrix $U = U_e^\dagger U_\nu$, where U_e and U_ν result from the diagonalisation of the charged lepton and neutrino mass matrices, we have analysed the sum rules which the Dirac phase δ present in U satisfies when U_ν has a form dictated by, or associated with, discrete symmetries and U_e has a "minimal" form (in terms of angles and phases it contains) that can provide the requisite corrections to U_ν, so that the reactor, atmospheric and solar neutrino mixing angles θ_{13}, θ_{23} and θ_{12} have values compatible with the current data.

In the scheme considered by us the four observables θ_{12}, θ_{23}, θ_{13} and the Dirac phase δ in the PMNS matrix are functions of three parameters θ_{12}^{e}, $\hat{\theta}_{23}$ and ϕ. As a consequence, the Dirac phase δ can be expressed as a function of the three PMNS angles θ_{12}, θ_{23} and θ_{13}, leading to a new "sum rule" relating δ and θ_{12}, θ_{23} and θ_{13}. This sum rule is exact within the scheme considered. Its explicit form depends on the symmetry form of the matrix $\tilde{U}_{\nu}$, i.e., on the value of the angle θ_{12}^{ν}. For arbitrary fixed value of θ_{12}^{ν} the sum rule of interest is given in eq. (5) [6]. A similar exact sum rule can be derived for the phase ϕ (eq. (6)) [6].

We show, in particular, that the exact sum rule predictions for $\cos\delta$ vary significantly with the symmetry form of $\tilde{U}_{\nu}$. This result implies that the measurement of $\cos\delta$ can allow us to distinguish between the different symmetry forms of $\tilde{U}_{\nu}$ [6] provided $\sin^2\theta_{12}$, $\sin^2\theta_{13}$ and $\sin^2\theta_{23}$ are known with a sufficiently good precision. Even determining the sign of $\cos\delta$ will be sufficient to eliminate some of the possible symmetry forms of $\tilde{U}_{\nu}$.

We find also that the exact sum rule predictions for $\cos\delta$ exhibit strong dependence on the value of $\sin^2\theta_{12}$ when the latter is varied in its 3σ experimentally allowed range (0.259 – 0.359). The predictions for $\cos\delta$ change significantly not only in magnitude, but in the cases of TBM, GRA and GRB forms of $\tilde{U}_{\nu}$ also the sign of $\cos\delta$ can change.

In all cases considered, having the exact sum rule results for $\cos\delta$, we could investigate the precision of the leading order sum rule predictions for $\cos\delta$. We found that the leading order sum rule predictions for $\cos\delta$ are, in general, imprecise and in many cases are largely incorrect, the only exception being the case of the BM (LC) form of $\tilde{U}_{\nu}$ [6].

Finally, we have performed a statistical analysis of the predictions for δ, $\cos\delta$ and the rephasing invariant $J_{\rm CP}$ which controls the magnitude of CPV effects in neutrino oscillations [23], in the cases of the TBM, BM (LC), GRA, GRB and HG symmetry forms of the matrix $\tilde{U}_{\nu}$ considered. In this analysis we have used as input the latest results on $\sin^2\theta_{12}$, $\sin^2\theta_{13}$, $\sin^2\theta_{23}$ and δ, obtained in the global analysis of the neutrino oscillation data performed in [22]. Our goal was to derive the allowed ranges for δ, $\cos\delta$ and $J_{\rm CP}$, predicted on the basis of the current data on the neutrino mixing parameters for each of the symmetry forms of $\tilde{U}_{\nu}$ considered. The results of this analysis are shown in Figs. 6 and 7. We have shown, in particular, that the CP-conserving value of $J_{\rm CP} = 0$ is excluded in the cases of the TBM, GRA, GRB and HG neutrino mixing symmetry forms, respectively, at approximately 5σ, 4σ, 4σ and 3σ confidence level with respect to the confidence level of the corresponding best fit values (Fig. 7). These results reflect the predictions we have obtained for δ, more specifically, the confidence levels at which the CP-conserving values of $\delta = 0$, π, 2π, are excluded in the discussed cases (see Fig. 6). We have found also that the 3σ allowed intervals of values of δ and $J_{\rm CP}$ are rather narrow for all the symmetry forms considered, except for the BM (LC) form. More specifically, for the TBM, GRA, GRB and HG symmetry forms we have obtained at 3σ: $0.020 \leq |J_{\rm CP}| \leq 0.039$. For the best fit values of $J_{\rm CP}$ we have found, respectively: $J_{\rm CP} = (-0.034)$, (-0.033), (-0.034), and (-0.031). Our results indicate that distinguishing between the TBM, GRA, GRB and HG symmetry forms of the neutrino mixing would require extremely high precision measurement of the $J_{\rm CP}$ factor.

The predictions for δ, $\cos\delta$ and $J_{\rm CP}$ in the case of the BM (LC) symmetry form of $\tilde{U}_{\nu}$, as the results of the statistical analysis performed by us showed, differ significantly from those found for the TBM, GRA, GRB and HG forms: the best fit value of $\delta \cong \pi$, and, correspondingly, of $J_{\rm CP} \cong 0$. For the 3σ range of $J_{\rm CP}$ we have obtained in the case of NO (IO) neutrino mass spectrum: -0.026 $(-0.025) \leq J_{\rm CP} \leq 0.021$ (0.023), i.e., it includes a sub-interval of values centred on zero, which does not overlap with the 3σ allowed intervals of values of $J_{\rm CP}$ in the TBM, GRA, GRB and HG cases.

The results obtained in the present study, in particular, show that the experimental measurement of the cosine of the Dirac phase δ of the PMNS neutrino mixing matrix can provide unique information about the possible discrete symmetry origin of the observed pattern of neutrino mixing.

Acknowledgements
I.G. would like to thank the organizers of the conference DISCRETE 2014 for the opportunity to present this study. This work was supported in part by the European Union FP7 ITN INVISIBLES (Marie Curie Actions, PITN-GA-2011-289442-INVISIBLES), by the INFN program on Theoretical Astroparticle Physics (TASP), by the research grant 2012CPPYP7 (*Theoretical Astroparticle Physics*) under the program PRIN 2012 funded by the Italian Ministry of Education, University and Research (MIUR) and by the World Premier International Research Center Initiative (WPI Initiative, MEXT), Japan (S.T.P.).

References

[1] K. Nakamura and S. T. Petcov, in K. A. Olive *et al.* (Particle Data Group), Chin. Phys. C **38** (2014) 090001.
[2] S. K. Agarwalla *et al.*, JHEP **1405** (2014) 094; C. Adams *et al.*, arXiv:1307.7335 [hep-ex]; A. de Gouvea *et al.*, arXiv:1310.4340 [hep-ex].
[3] S.M. Bilenky, J. Hosek and S.T. Petcov, Phys. Lett. B **94** (1980) 495.
[4] P. Langacker *et al.*, Nucl. Phys. B **282** (1987) 589.
[5] D. Marzocca, S. T. Petcov, A. Romanino and M. C. Sevilla, JHEP **1305** (2013) 073.
[6] S. T. Petcov, Nucl. Phys. B **892** (2015) 400.
[7] S. Antusch and S. F. King, Phys. Lett. B **631** (2005) 42.
[8] S. F. King, JHEP **0508** (2005) 105.
[9] S. F. King *et al.*, New J. Phys. **16** (2014) 045018.
[10] S. F. King and C. Luhn, Rept. Prog. Phys. **76** (2013) 056201.
[11] I. Girardi, S. T. Petcov and A. V. Titov, Nucl. Phys. B **894** (2015) 733.
[12] P. F. Harrison, D. H. Perkins and W. G. Scott, Phys. Lett. B **530** (2002) 167; P. F. Harrison and W. G. Scott, Phys. Lett. B **535** (2002) 163; Z. z. Xing, Phys. Lett. B **533** (2002) 85; X. G. He and A. Zee, Phys. Lett. B **560** (2003) 87; see also L. Wolfenstein, Phys. Rev. D **18** (1978) 958.
[13] S. T. Petcov, Phys. Lett. B **110** (1982) 245.
[14] F. Vissani, hep-ph/9708483; V. D. Barger, S. Pakvasa, T. J. Weiler and K. Whisnant, Phys. Lett. B **437** (1998) 107; A. J. Baltz, A. S. Goldhaber and M. Goldhaber, Phys. Rev. Lett. **81** (1998) 5730.
[15] L. L. Everett and A. J. Stuart, Phys. Rev. D **79** (2009) 085005.
[16] Y. Kajiyama, M. Raidal and A. Strumia, Phys. Rev. D **76** (2007) 117301.
[17] W. Rodejohann, Phys. Lett. B **671** (2009) 267; A. Adulpravitchai, A. Blum and W. Rodejohann, New J. Phys. **11** (2009) 063026.
[18] C. H. Albright, A. Dueck and W. Rodejohann, Eur. Phys. J. C **70** (2010) 1099.
[19] J. E. Kim and M. S. Seo, JHEP **1102** (2011) 097.
[20] I. Girardi, A. Meroni, S. T. Petcov and M. Spinrath, JHEP **1402** (2014) 050.
[21] M. C. Chen and K. T. Mahanthappa, Phys. Lett. B **681** (2009) 444; M. C. Chen, J. Huang, K. T. Mahanthappa and A. M. Wijangco, JHEP **1310** (2013) 112.
[22] F. Capozzi *et al.*, Phys. Rev. D **89** (2014) 093018.
[23] P. I. Krastev and S. T. Petcov, Phys. Lett. B **205** (1988) 84.